CO_2 PROFILING BY SPACE-BORNE RAMAN LIDAR

Paolo Di Girolamo[1*], Carmine Serio[1], Volker Wulfmeyer[2], Andreas Behrendt[2], Davide Dionisi[3]

[1]*Scuola di Ingegneria, Università della Basilicata, Potenza, Italy*
[2]*Institut fuer Physik und Meteorologie, Universitaet Hohenheim, Stuttgart, Germany*
[3]*ISMAR,CNR, Roma, Italy*
**Email: paolo.digirolamo@unibas.it*

ABSTRACT

As clearly reported in the IPCC fifth Assessment Report, CO_2 emissions are already producing destructive effects to the plant ecosystem through the alteration of soil-atmosphere interaction mechanisms.

Although the space and ground network for CO_2 monitoring has regularly expanded over the past 50 years, it does not guarantee the necessary spatial and temporal resolution needed for a quantitative analysis of sources and sinks. For the purpose of estimating forests' carbon capturing capabilities, accurate measurements of CO_2 gradients between the forest floor and the top of the canopy, which ultimately translates into the capability to measure CO_2 concentration profiles. Space sensors provide CO_2 measurements above forest canopies, which do not allow to properly estimate Gross Primary Production (GPP).

These observational gaps could be addressed with an active remote sensing system in space based on the vibrational Raman lidar technique. CO_2 profile measurements are possible, together with simultaneous measurements of the temperature and water vapour mixing ratio profile and a variety of additional variables (aerosol backscatter profile, aerosol extinction profile, PBL depth, cloud top and base heights, cloud optical depth). An assessment of the expected performance of the system has been performed based on the application of an analytical simulation model developed at University of Basilicata.

1. INTRODUCTION

Global warming is a consequence of the alteration of Earth's natural greenhouse effect. More than 75 % of this effect is dominated by water vapour, while the remaining 25 % primarily by CO_2. While human activities modify the Earth's hydrological cycle in a minor extent, they substantially alter the carbon cycle: CO_2 mixing ratio in the atmosphere has substantially increased from values around 300 ppm in the fifties to a current value exceeding 405-410 ppm, with an annual increasing rate of approximately 2 ppm.

Approximately half of CO_2 amount produced through fossil fuel combustion and other human activities is injected in the atmosphere and accumulates in it. The remaining part is absorbed by the oceans and the terrestrial biosphere (e.g. [1]). An appropriate quantitative assessment of the various components of the carbon cycle requires accurate measurements of the different sources and sinks and, ultimately, of chlorophyll vegetation photosynthesis, i.e. the Gross Primary Productivity or GPP.

Forests cover ~30% of the Earth's global land area [2]. Forests store large amounts of carbon captured from the atmosphere and retained in living and dead biomass and soil. The estimated amount of carbon dioxide (CO_2) in the atmosphere is equivalent to an amount of carbon of 8×10^{14} kg, while the amount stored in terrestrial biomass is 5×10^{14} kg, 60% of which (3×10^{14} kg) being stored in forest systems [3]. The missing balance between the carbon released in the atmosphere through the combustion of fossil fuels and deforestation on one side, and the uptake by sinks in oceanic and terrestrial systems on the other side has led to the 2 ppm per year increase in atmospheric CO_2 concentration mentioned at the beginning of this section.

Based on the above considerations, it appears clear that accurate measurements of CO_2 gradients between the forest floor and the top of the canopy, and their temporal variations, are urgently needed. These measurements are of paramount importance for an appropriate assessment of the potential impact of increased atmospheric CO_2 on ecosystems and for the characterization of coupling processes between the forest and the convective boundary layer.

Our current knowledge about atmospheric CO_2 concentrations and surface fluxes at regional scales over the globe comes primarily from ground-based in situ measurements from air

sampling networks and tall towers [4]. However, due to the sparseness of such measurements, there are still large uncertainties especially on the surface fluxes [5].

CO_2 measurements based on the application of the vibrational Raman lidar technique have been carried out since the early nineties [6-7]. Despite its high potential impact, the Raman lidar technique for CO_2 measurements has received limited attention in the last 25 years both at theoretical and experimental level, mainly because of its limited precision resulting from the small cross-section of vibrational Raman scattering and the low CO_2 concentration.

However, in the last decade, considerable technological advances have been achieved in the design and development of high-power solid-state laser sources, large-aperture telescopes and high gain/quantum efficiency detectors. These advances allow today reaching a new level of performance in CO_2 Raman lidar measurements from both ground and space platforms.

In the present paper, system performance in terms of measurement precision of space-borne CO_2 Raman lidar has been estimated based on the application of an analytical simulator developed at Univ. of Basilicata [8,9].

2. METHODOLOGY

2.1 CO_2 vertical variability

The seasonal and annual mean of CO_2 vertical profile reflect the combined influences of surface fluxes and atmospheric mixing. In the Northern Hemisphere, during the summer season, midday atmospheric CO_2 concentrations are generally lower near the surface than in the free troposphere, reflecting the higher impact of terrestrial photosynthesis over industrial emissions [5]. Conversely, during the winter, respiration and fossil-fuel sources lead to elevated low-altitude atmospheric CO_2 concentrations. The gradients are comparable in magnitude in both seasons, but the positive gradients persist for a larger portion of the year, leading to annual-mean gradients also showing higher atmospheric CO_2 concentrations near the surface than aloft [5]. The average midday differences in the Northern Hemisphere between 1 and 4 km, expressed in terms of CO_2 mixing ratio, is –2.2 ppm in summer, +2.6 ppm in winter, while instantaneous differences may be as large as 5-10 % [10]. The Southern Hemisphere locations show relatively constant CO_2 profiles in all seasons, with slightly higher values in the free troposphere [5]. Similar gradients are found in the NOAA's Carbon Tracker version 2010 [4].

CO_2 gradients between the forest floor and the top of the canopy range between 75 and 100 ppm at night, compared to 10-50 ppm during the day. Both ranges represented spring conditions when canopy leaf area development is not completed [11].

2.2 The lidar system

The Raman lidar technique has proved to be very effective in the profiling of atmospheric thermodynamic and compositional properties [12,13,14]. The Raman lidar BASIL has been deployed in a variety of international field experiments [15,16,17,18,19,20,21].

The lidar setup considered in the present research effort relies heavily on the ATLAS mission concept [9] which was submitted to the European Space Agency as part of the Earth Explorer-10 Call. Simulations consider a sun-synchronous low Earth orbit, with an orbiting height and speed of 450 km and 7 km/s, respectively. A dawn-dusk orbit with overpasses at 6/18 h local time has been selected for the simulations.

The lidar transmitter consists of a frequency-tripled, diode-laser pumped Nd:YAG laser, with an an average power in the UV (at 354.7 nm) of 250 W (single pulse energy = 2.5 J, repetition rate = 100 Hz). An electrical-to-optical efficiency > 5 % is assumed in order to achieve such high laser power based on the available on-board electrical power. The receiver consists of a large-aperture telescope, with a primary-mirror diameter of 4 m, and a high efficiency receiving unit for the collection of the Raman signals. Receiving field-of-view (FWHM) is 10 μrad. The present mission concept considers a Raman lidar system collecting five primary lidar signals: the CO_2 vibrational and water vapour roto-vibrational Raman signals, $P_{CO2}(z)$ and $P_{H2O}(z)$, respectively, the high- and low-quantum number rotational Raman signals, $P_{LoJ}(z)$ and $P_{HiJ}(z)$, and the elastic backscatter signal at λ_0, $P_{\lambda 0}(z)$.

The spectral selection is performed through the use of narrow-band interference filters (IFs). Specifically, the IFs are used to select the Q-branch of the two bands v_1 and $2v_2$ both in the Stokes and anti-Stokes branches of CO_2

vibrational Raman band. IFs have central wavelengths (CWLs) of 338.1, 339.2, 371.71 and 373.1 nm, bandwidths of 0.1 nm, transmissions at CWLs of 80%, out of band rejections of OD6 @ 200-1200 nm, OD12 @ 354.7 nm and OD7 @ 325-340 and 370-390 and nm. Reported simulations consider photon detection by accumulation charge-coupled devices (ACCDs), with UV quantum efficiencies of 85%.

The central wavelength of the CO_2 band is almost coincident with the twenty-first anti-Stokes roto-vibrational O_2 line, which represents a potential source of contamination for CO_2 Raman lidar measurements [12]. Riebesell [6] and Ansmann et al. [7] came to the conclusion that CO_2 Raman lidar measurements were hardly feasible due to the difficulties in accurately estimating the magnitude of the interference by O_2 rotational lines. These authors also argued that fluorescence generated by either the receiver optics or atmospheric particles could potentially prevent from reaching a measurement accuracy at the 1 ppm level.

However, these early research efforts were conducted using excimer laser sources (Xe:Cl mixture), which have an emission spectrum typically spanning over a spectral interval of ~0.4 nm. Such broad spectrum makes separation of CO_2 and O_2 lines more difficult with respect to what is presently achievable based on the use of narrowband interference filters (0.1 nm) and injection-seeded Nd:YAG laser sources (typical spectral width of ~0.01 nm). Whiteman et al. [12] demonstrated that the bias affecting CO_2 measurements as a result of the contamination by the 21st O_2 rotational line is not exceeding 1 % if a 0.1-nm wide IF and a narrow-band Nd:YAG laser source (<0.02 nm) are used. Based on an appropriate rotational strength modeling as a function of temperature and relying on independent temperature profile measurements provided by the same lidar system, the magnitude of the interference can be properly estimated and subtracted from the CO_2 signal so that a residual systematic uncertainty of the order of 0.1-0.2 ppm is left in CO_2 mixing ratio measurements.

3. RESULTS

3.1 Input data for the Simulator

An appropriate input CO_2 mixing ratio profile was generated which accounts for different vertical gradients associated with the conflicting contributions of terrestrial photosynthesis and industrial emissions, and CO_2 capturing within forest canopy.

This input profile includes a 5 ppm increase at an altitude of 2 km (from a value of 405 to one of 410 ppm), introduced in order to simulate the daytime CO_2 depletion taking place within the mixed layer. In addition to this, a 50 ppm decrease is considered at an altitude of 50 m above the surface level, which is intended to represent CO_2 capturing within forest canopy.

Atmospheric quantities considered in the simulation include vertical profiles of pressure, temperature, and humidity from the U.S. Standard Atmosphere 1976 atmospheric reference model. Aerosol optical properties are simulated based on the use of the median aerosol extinction data from the ESA ARMA Model [22].

3.2 Simulation results

Considering vertical and horizontal resolutions of 200 m and 200 km, respectively, the statistical uncertainty affecting CO_2 mixing ratio profile measurements is not exceeding 2 ppm at night and 10 ppm in daytime from the surface up to an altitude of 5 km, with slightly higher values in the vertical region from the forest floor to the top of the canopy (Fig. 1). Ground-based demonstrations of the present instrument concept are under implementation both at Univ. of Basilicata and Univ. of Hohenheim.

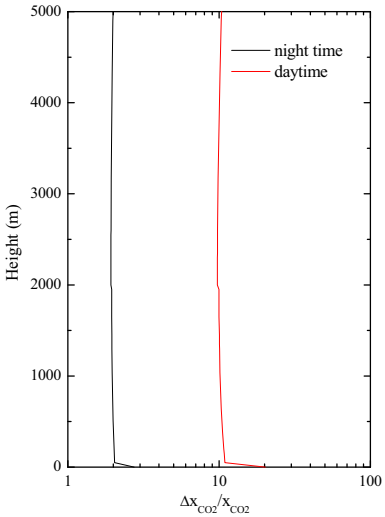

Figure 1: CO_2 mixing ratio profiling precision (in %). The black line represents night-time performance, while the red line represents daytime performance.

ACKNOWLEDGEMENTS

This work was supported by the Italian Ministry for Education, University and Research under the Grant OT4CLIMA.

REFERENCES

[1] C. Le Quéré *et al.*, The global carbon budget 1959–2011, Earth Syst. Sci. Data, 5, 165–185 (2013).
[2] G.J. Nabuurs et al., Forestry. In Climate Change 2007: Mitigation. Contribution of Working Group III to the Fourth Assessment Report of the Intergovernmental Panel on Climate Change, Cambridge University Press, Cambridge, UK and New York, NY (2007).
[3] D.C. McKinley *et al.*, A synthesis of current knowledge on forests and carbon storage in the United States, Ecol. App., doi:10.1890/10-0697.1 (2011).
[4] M. Reuter *et al.*, A simple empirical model estimating atmospheric CO_2 background concentrations, Atmos. Meas. Tech., 5, 1349–1357 (2012).
[5] B. B Stephens *et al.*, Weak Northern and Strong Tropical Land Carbon Uptake from Vertical Profiles of Atmospheric CO_2, Science, 316, 1732-1735 (2007).
[6] M. Riebesell, Raman lidar for the remote sensing of the water vapor and carbon dioxide profile in the troposphere (in German). Ph.D. thesis, GKSS document 901/F/13, University of Hamburg, 127 pp. (1990).
[7] A. Ansmann *et al.*, Combined Raman Elastic-backscatter lidar for vertical profiling of moisture, aerosol extinction, backscatter, and lidar ratio, Appl. Phys., 55B, 18-28 (1992).
[8] P. Di Girolamo *et al.*, Spaceborne profiling of atmospheric temperature and particle extinction with pure rotational Raman Lidar and of relative humidity in combination with differential absorption Lidar: performance simulations. Applied Optics, 45, 2474-2494, doi: 10.1364/AO.45.002474 (2006).
[9] P. Di Girolamo *et al.*, Space-borne profiling of atmospheric thermodynamic variables with Raman lidar: performance simulations, Optics Express, 26(7), 8125-8161, doi: 10.1364/OE.26.008125 (2018).
[10] Gatti et al., Vertical profiles of CO2 above eastern Amazonia suggest a net carbon flux to the atmosphere and balanced biosphere between 2000 and 2009, Tellus, 62B, 581–594 *(*2010).
[11] Buchmann et al., Global Change Biology, 2**,** 421-432, 1996.
[12] P. Di Girolamo *et al.*, Rotational Raman Lidar measurements of atmospheric temperature in the UV. Geophysical Research Letters, 31, doi: 10.1029/2003GL018342 (2004).
[13] D. N. Whiteman *et al.*, Demonstration Measurements of Water Vapor, Cirrus Clouds, and Carbon Dioxide using a High-Performance Raman Lidar**,** Journal of Atmospheric and Oceanic Technology, 24, 1377-1388 (2007).
[14] P. P. Di Girolamo *et al.*, Multiparameter Raman Lidar Measurements for the Characterization of a Dry Stratospheric Intrusion Event, Journal of Atmospheric and Oceanic Technology, 26, 1742-1762, doi: 10.1175/2009JTECHA1253.1 (2009).
[15] Bhawar *et al.*, Spectrally Resolved Observations of Atmospheric Emitted Radiance in the H_2O Rotation Band, Geophysical Research Letters, 35, L04812, ISSN: 0094-8276, doi: 10.1029/2007GL032207 (2008).
[16] Serio *et al.*, Retrieval of foreign-broadened water vapor continuum coefficients from emitted spectral radiance in the H2O rotational band from 240 to 590 cm-1, Optics Express, 16/20, 15816-15833, doi: 10.1364/OE.16.015816 (2008).
[17] Wulfmeyer *et al.*, Research campaign: The convective and orographically induced precipitation study - A research and development project of the World Weather Research Program for improving quantitative precipitation forecasting in low-mountain regions, Bulletin of the American Meteorological Society, 89, 1477-1486, ISSN: 0003-0007, doi: 10.1175/2008BAMS2367.1 (2008).
[18] Bennett *et al.*, Initiation of convection over the Black Forest mountains during COPS IOP15a, Quarterly Journal of the Royal Meteorological Society, 137, 176-189, doi: 10.1002/qj.760 (2011).
[19] Kiemle *et al.*, Latent heat flux measurements over complex terrain by airborne water vapour and wind Lidars. Quarterly Journal of the Royal Meteorological Society, 137, 190-203, ISSN: 0035-9009, doi: 10.1002/qj.757 (2011).
[20] Steinke et al., Assessment of Small-Scale Integrated Water Vapour Variability During HOPE, Atmospheric Chemistry and Physics, 15(5), 2675-26929, doi:10.5194/acp-15-2675-2015 (2015).
[21] Macke *et al.*, The HD(CP)2 Observational Prototype Experiment HOPE - An Overview, Atmospheric Chemistry and Physics, 17, 4887–4914, doi:10.5194/acp-17-4887-2017 (2017).
[22] ESA, "ARMA Reference Model of the Atmosphere," in Technical Report APP-FP/99–11239/AC/ac (European Space Agency, 1999).